



THE ANTIBACTERIAL ACTIVITY OF TiO₂ NANOPARTICLES PREPARED BY SOL-GEL METHOD FOR A GROUP OF GRAM-POSITIVE AND NEGATIVE BACTERIA

Mayes. Mohammad Tayeh^{1*}, Lamees Thamer AL- hadedee²

¹Department of Food Science, College of Agricultural Engineering Sciences, University of Baghdad, Iraq. mais.mohammed1202a@coagri.uobaghdad.edu.iq

²Assistant Professor PhD. Department of Food Science, College of Agricultural Engineering Sciences, University of Baghdad, Iraq. lames.thamer@coagri.uobaghdad.edu.iq

Received 19/ 2/ 2023, Accepted 6/ 7/ 2023, Published 30/ 6/ 2024

This work is licensed under a CCBY 4.0 <https://creativecommons.org/licenses/by/4.0>



ABSTRACT

Titanium dioxide nanoparticles TiO₂ NP were prepared by sol-gel method. TiO₂ NP was identified and characterized using scanning electron microscopy (SEM), ultraviolet spectroscopy (UV-vis), Fourier transform infrared (FTIR), X-ray diffraction (XRD) and atomic force microscopy (AFM). The SEM results showed an irregular spherical shape with different diameters (22.84-65.98) nm. The highest UV-Vis absorption was recorded at 345 nm wavelength. FTIR was used to find out the effective aggregates and the success of the process of forming TiO₂ NP bands. The first centered between (450 – 800 cm⁻¹), which is attributed to the patterns of stretching vibrations of the titanium oxide bond (Ti-O Vibrations). While the XRD peaks appeared at angles 2θ (27.32°, 35.89°, 39.03°, 41.02°, 43.88°, 54.09°, 56.38°, 62.43°, 63.77°, 68.67°, 69.41°, 76.11°) at Crystal Planes (110) (101) (200) (111) (210) (211) (220) (002) (310) (301) (112) and (202), (respectively, which corresponds to JCPDS standard tables), and this indicates the formation of rutile-type NPs TiO₂. The results of (AFM) ranged between (6-7 nm) and the mean height (Z-mean value) was (8 nm). The effectiveness of NP TiO₂ was tested at different concentrations (1, 0.75, 0.5) mg/ml against a group of Gram-negative and Gram-positive bacteria: (*Pseudomonas aeruginosa*, *Salmonella typhimurium*, *Bacillus subtilis*, *Staphylococcus aureus*, *E.coli*) reached the highest zone of inhibition at a concentration of (1) mg/ml for *Staphylococcus aureus*, as the diameter of inhibition was (19.5).

Keywords: TiO₂, minimum inhibition, sol gel, Nanoparticles

*The research is taken from a master's thesis by the first researcher.

الفعالية المضادة لجسيمات التيتانيوم النانوية المحضرة بطريقة السول-جل لمجموعة من البكتريا السالبة و الموجبة لصبغة كرام

ميس محمد تايه¹ ، لميس ثامر الحديدي²

¹قسم علوم الأغذية، كلية علوم الهندسة الزراعية، جامعة بغداد، بغداد، العراق، mais.mohammed1202a@coagri.uobaghdad.edu.iq

²الاستاذ المساعد الدكتور، قسم علوم الأغذية، كلية علوم الهندسة الزراعية، جامعة بغداد، بغداد، العراق، ames.thamer@coagri.uobaghdad.edu.iq

الخلاصة

تم تحضير ثاني أكسيد التيتانيوم النانوي TiO_2 NP بواسطة طريقة السول-جل، حيث تم تشخيص وتوصيف TiO_2 NP باستخدام المجهر الإلكتروني الماسح (SEM)، مطياف الأشعة فوق البنفسجية (UV-vis)، تحويل فوريير الأشعة تحت الحمراء (FTIR)، حيود الأشعة السينية (XRD) ومجهر القوة الذرية (AFM). أظهرت نتائج (SEM) شكلاً كروي (Spherical Shape) غير منتظم و بأقطار مختلفة بلغت (65.98-22.84) nm. وبلغ أعلى امتصاص لـ UV-Vis سجله عند الطول الموجي 345 nm. واستخدم (FTIR) لمعرفة المجاميع الفعالة ومدى نجاح عملية تكوين TiO_2 NP الحزمة الأولى تتمركز بين ($450 - 800 \text{ cm}^{-1}$) والتي تعزى إلى انماط اهتزازات التمدد (Stretching Vibrations) لاصرة أكسيد معدن التيتانيوم Ti-O. في حين XRD ظهر قمم عند الزوايا

$(27.32^\circ, 35.89^\circ, 39.03^\circ, 41.02^\circ, 43.88^\circ, 54.09^\circ, 56.38^\circ, 62.43^\circ, 63.77^\circ, 68.67^\circ, 69.41^\circ, 76.11^\circ)$ عند المستويات البلورية (110) (101) (200) (111) (210) (211) (220) (002) (310) (301) (112)

و(202) على التوالي والذي يتطابق مع الجداول القياسية (JCPDS) وهذا يشير على تكوين TiO_2 NP من نوع روتيل.

أما نتائج (AFM) كانت تتراوح بين (6-7 nm) ومعدل ارتفاع (Z-mean value) (8 nm). أُختبرت فعالية TiO_2 NP بتركيز مختلفة (0.5, 1, 0.75) ملغم/مل ضد مجموعة من البكتريا السالبة والموجبة لصبغة كرام

(*Bacillus subtilis*, *Staphylococcus aureus*, *Escherichia coli*, *Salmonella typhimurium*)

Pseudomonas aeruginosa)

بلغت أعلى منطقة تثبيط عند تركيز (1) ملغم/مل مل لبكتريا *Staphylococcus aureus* إذ كان قطر التثبيط

(19.5).

الكلمات المفتاحية: ثاني أكسيد التيتانيوم، أقل فعالية تثبيطية، سول-جل، جزيئات النانو.

INTRODUCTION

TiO_2 NP is a semiconductor transition metal oxide that exhibits unique properties such as low cost, ease of handling, non-toxicity and resistance to chemical corrosion. These advantages make TiO_2 NP a widely used material in solar cells, chemical sensors, self-cleaning surfaces, environmental cleaning applications and in the food industry (Hamza et al., 2013). TiO_2 NP exists in both crystalline and amorphous forms and is mainly found in three polymorphic forms namely anatase, rutile and brookite. Anatase and rutile have a quadrangular structure, while brookite has a straight structure (Jafer et al, 2009) Crystal phase, particle size, and particle shape all influence the physical and chemical characteristics of TiO_2 (Fahem et al., 2022). There are different methods that can be used to synthesize TiO_2 NP (Kim et al., 2004) such as spraying, chemical vapor deposition, microwaves and method Sol-gel (Di Paole et al., 2013) which is one of the most promising technologies as this method Homogeneous samples at low cost produces (Dai et al. , 2010).

MATERIAL AND METHODS

Preparation of TiO₂ NP by sol-gel method

TiO₂ NP was prepared by the sol-gel method by dissolving 12ml of titanium tetraisopropoxide (TTIP) in 100ml of ethanol and stirring the mixture for 30 minutes using a magnetic stirrer, 3ml of deionized water and 2ml of HCl were added into the solution drip and continued stirring for two hours to obtain a homogeneous solution at a pH of (3), then the solution was left for 24 hours, after which the gel was dried at 400 °C (Ramalingam *et al*, 2019).

Diagnosis and characterization of TiO₂ NP

The characterization process was carried out using a scanning electron microscope (SEM), a UV-visible spectrometer (UV), Fourier transform spectroscopy (FTIR), X-ray diffraction (XRD), and Atomic Force Microscopy (AFM) .

TiO₂ NP's minimum inhibitory concentration Test (MIC)

The Agar well diffusion method mentioned by (De Oliveira *et al.*, 2014) was followed, where the inhibition activity of TiO₂ NP was tested against the isolates used in the study by growing the isolates in 10 ml of the nutrient broth prepared at 37 °C for 24 hours (Al-hadedee & Awahd, 2022), then spreading 0.1 ml of activated test bacteria on the surface of the a solid culture medium Muller Hinton Agar using a sterile glass diffuser (L-shape), a hole with diameter of 6 mm was made on the surface of the culture medium with a corkscrew, and 50 of microliters of the solution was placed in each hole with concentrations of (1, 0.75, 0.5) mg /ml TiO₂ NP using a micropipette, then the plates were incubated at a temperature of 37 °C for 24 hours in the incubator, then the diameter of the corona was Measured Inhibition Zone.

Organisms used

E. coli, *Pseudomonas aeruginosa*, *Salmonella typhimurium* *Bacillus subtilis*,
Staphylococcus aureus

RESULTS AND DISCUSSION

Diagnosis and characterization: SEM

(Figure, 1) shows the scanning electron microscopy images (FESEM Images) of the prepared TiO₂ NP at (100 kx and 200 kx) magnifications. The obtained results showed that the TiO₂ NP has a spherical shape. The average particle size ranges from 22.84-65.98 nm. And the difference in the size of the material in one sample indicates that it was formed at different times (Geethalakshmi & Sarada, 2012).

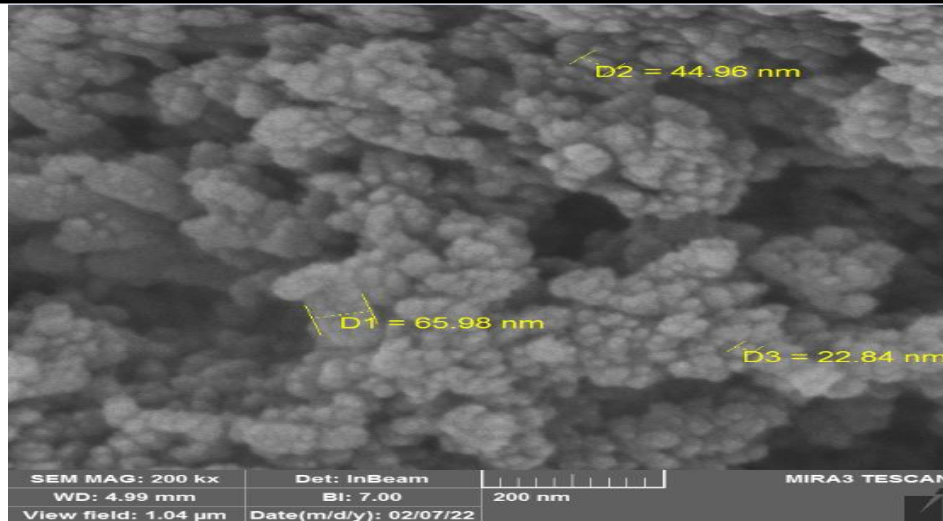


Figure (1): SEM images of TiO₂ NP

UV-visible spectrometer

Figure (2) shows the absorption spectrum of (TiO₂ NP) nanopowder prepared by the (sol-gel method). The results showed obtaining a prominent peak in the absorption spectrum at wavelength (345 nm) with an absorbance less than 1. Obtaining a strong peak at wavelength (345 nm) is within the wavelength range (200-1000 nm) confirms obtaining (TiO₂ NP) by the sol-gel method (Vijayalakshmi & Rajendran, 2012).

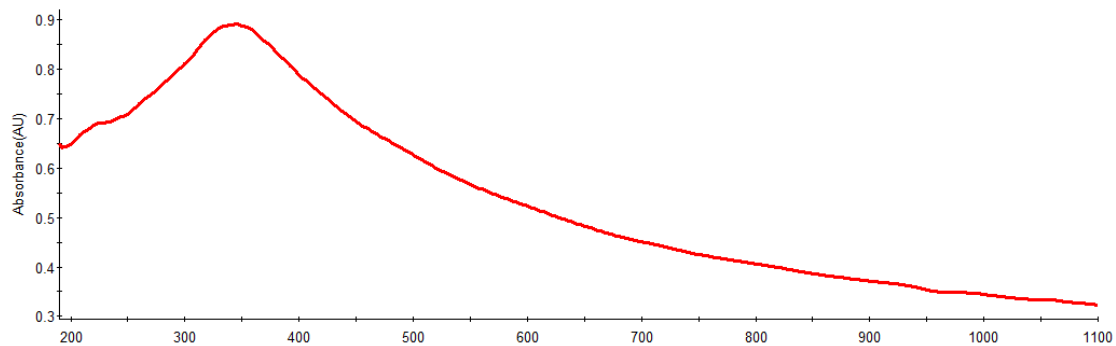


Figure (2): UV-Vis absorption spectral TiO₂ NP

Fourier transform spectroscopy (FTIR):

(Figure, 3) shows an Fourier transform spectroscopy (FTIR) examination of the prepared TiO₂ NP in order to determine the effective aggregates using the spectrometer (Shimadzu Japan-IR Affinity-1), by measuring the transmittance spectrum as a function of the wavenumber. number) within the range (400-4000 cm⁻¹). The results showed the emergence of three diagnostic bands (Characteristic Bands), the first band is centered between (450-800 cm⁻¹), which is attributed to the patterns of stretching vibrations of Ti-O Vibrations (Sonali *et al.*, 2021; Yu *et al.*, 2006), the second band is centered around (1636 cm⁻¹), which is due to the stretching vibrations of the (carboxyl-titanium) and hydroxyl (O-H) groups, respectively (Ghaly *et al.*, 2011), while the third band It is represented by a broad band centered between (3000 - 3800 cm⁻¹), which is due to the stretching vibrations of the

hydroxyl group (O-H) resulting from the moisture absorbed from the external environment by the prepared TiO₂ NP(Sonali *et al.*, 2021).

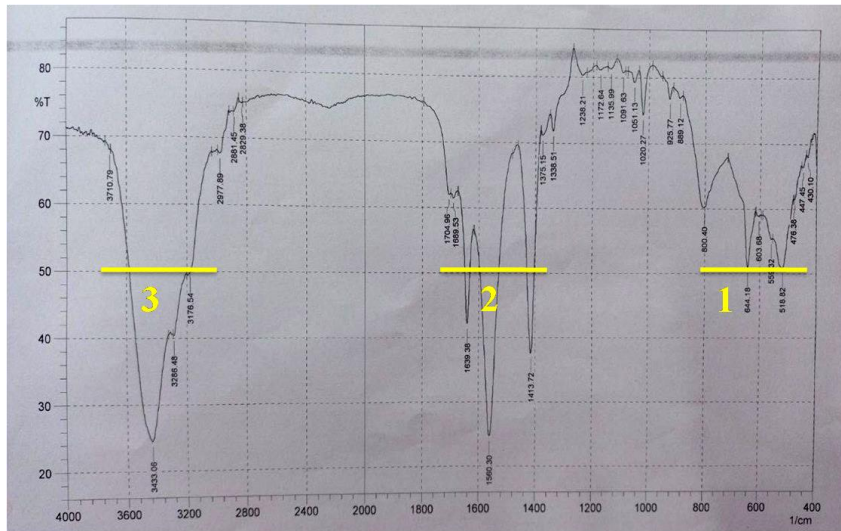


Figure (3): shows the FTIR spectrum diagram of TiO₂ NP particles

X-ray diffraction (XRD):

X-ray diffraction (XRD) of TiO₂ NP (Fig. 4) was carried out using an X-ray diffraction device (Shimadzu-6000) with a wavelength ($\lambda = 1.54060 \text{ \AA}$) and a potential difference (40 KV). The results of the X-ray diffraction (XRD) test showed that the diagnostic peaks were obtained Characteristic Peak of TiO₂ NPs at angles ($2\theta = 27.32^\circ, 35.89^\circ, 39.03^\circ, 41.02^\circ, 43.88^\circ, 54.09^\circ, 56.38^\circ, 62.43^\circ, 63.77^\circ, 68.67^\circ, 69.41^\circ, 76.11^\circ$) at Crystal Planes (110) (101) (200) (111) (210) (211) (220) (002) (310) (301) (112) and (202), respectively, which indicate obtaining (TiO₂ NPs) type rutile with a tetragonal crystal structure of (Space Group) level (P42/mnm no.136), with dimensions ($a = b = 4.6107 \text{ \AA}$ and $c = 2.9732 \text{ \AA}$) and crystal angles ($\alpha = \beta = \gamma = 90^\circ$), which corresponds to the standard card (JCPDS 01-077-0443). No other additional peaks were detected, which indicates obtaining high purity TiO₂ NPs.

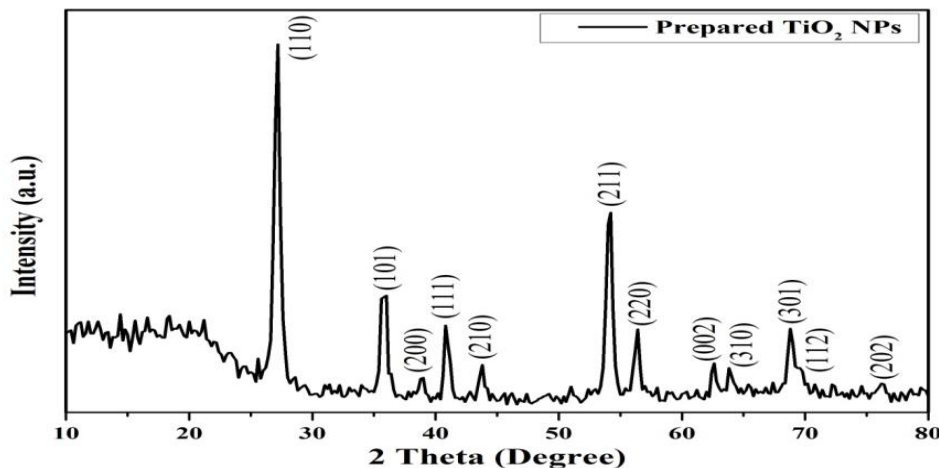


Figure (4): (XRD) TiO₂ NP prepared by (Sol-gel) method.

Atomic Force Microscopy AFM:

The surface morphology of the TiO₂ NP was studied by atomic force microscopy (AFM). Figure (a, b5) presents 2D and 3D atomic force microscope (AFM) images of TiO₂ nanoparticles prepared at (400 °C). The images showed that the TiO₂ NP powder has a high roughness surface with a granular microstructure and a non-flat texture, which consists of particles with diameters ranging between (6-7 nm) and a mean height (Z-mean value) of (8 nm), as shown in Figure (3). On the other hand, the atomic force microscopy (AFM) examination gives surface roughness values, as the root mean square (Sq) of TiO₂ NP is higher than (1 nm) with a value of (2.045 nm), and this indicates roughness High surface.

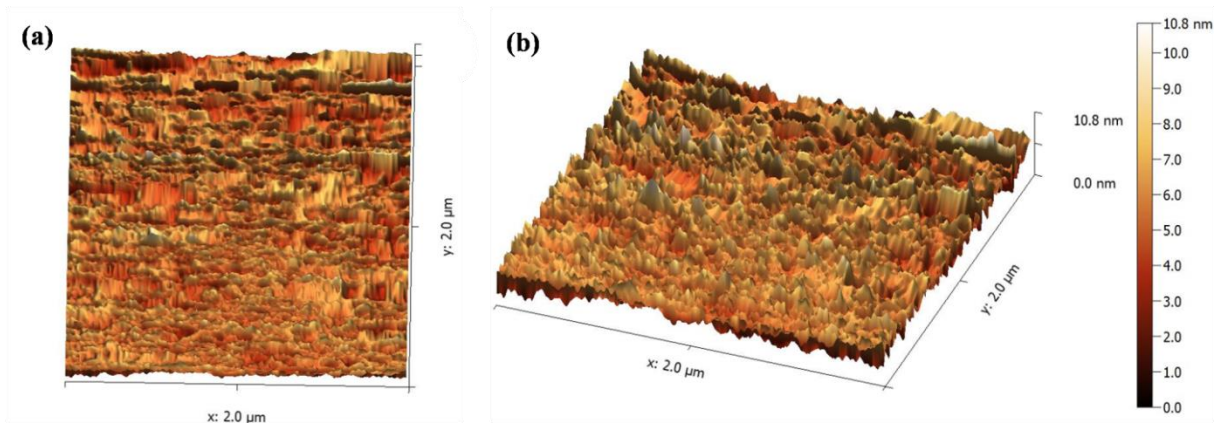


Figure (5): AFM images (a) 2D and (b) 3D of prepared and calcined NPs TiO₂ at (400 °C).

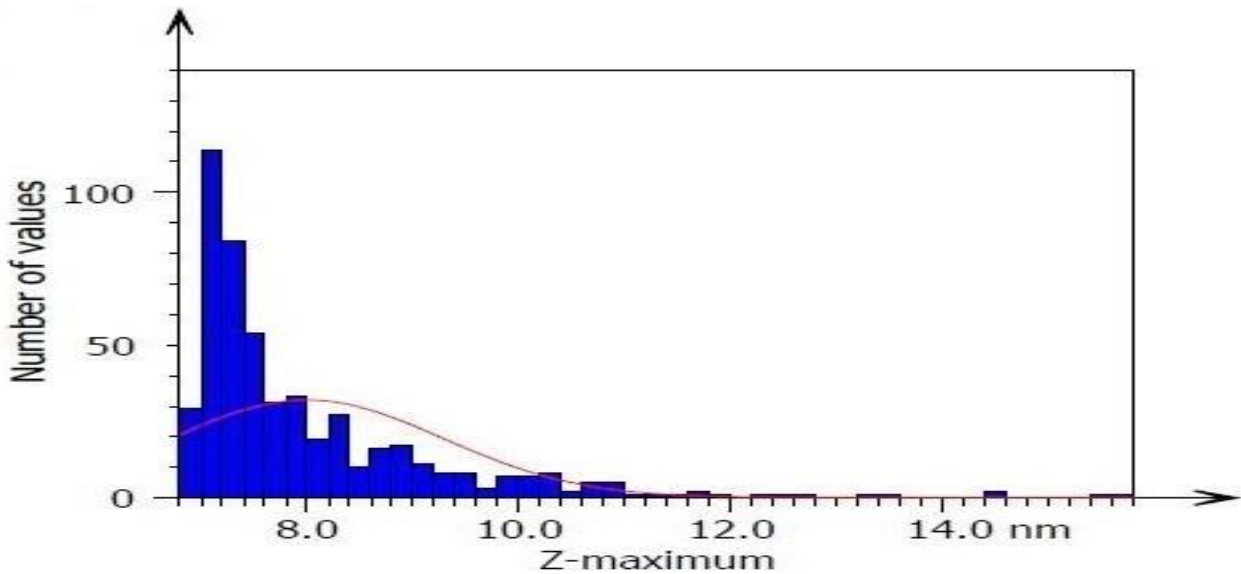


Figure (6): Z-mean value plot of the as-prepared TiO₂NPs

NP's minimum inhibitory concentration Test (MIC): TiO₂

The minimum inhibitory concentration (MIC) was determined by Agar well diffusion method at different concentrations (1, 0.75, 0.5) mg/ml. Its effect on inhibiting the growth of a group of bacteria was studied, some of which are Gram-positive and Gram-negative. The

results showed that the use of NP TiO₂ inhibited all types of bacteria Where the lowest value of the minimum inhibitory concentration was (0.5) mg/ml for Bacillus subtilis, as the diameter of inhibition was 9 mm, while the diameter of inhibition was (15.5, 13.5) mm, respectively, for the concentrations used (1,0.75) mg/ml. While the value of the minimum inhibitory concentration was (0.5) mg/ml for Staphylococcus aureus, and the diameter of inhibition was 9.5 mm, while the diameter of inhibition was (14.5, 19.5) mm, respectively, for the concentrations used (1, 0.75) mg/ml. As for the lowest value of the minimum inhibitory concentration was (0.5) mg/ml for E. coli bacteria, as the diameter of inhibition was 10 mm, while the diameter of inhibition was (17.5, 14) mm, respectively, for the concentrations used (1,0.75) mg/ml. The reason for the difference in inhibition on the types of positive and negative bacteria (Ahmad *et al.*,2015) where they found that NP TiO₂ invade bacterial cells by damaging the cell membrane in both positive and negative bacteria, causing cell leakage and death. And that the lowest value of the minimum inhibitory concentration was (0.5) mg/ml for Pseudomonas aeruginosa bacteria, as the diameter of inhibition was 10 mm, while the diameter of inhibition was (15.5,14) mm, respectively, for the concentrations used (1,0.75) mg/ml. While the lowest value for concentration the minimum inhibitor was (0.5) mg / ml for Salmonella typhimurium, as the diameter of inhibition was 9 mm, while the diameter of inhibition was (16,13.5) mm, respectively, for the concentrations used (1,0.75) mg / ml. The reason for the inhibition of gram-negative bacteria is due to the gram stain because the bacterial cells and the TiO₂ NP has opposite charges, whereby electrostatic attraction occurs between TiO₂ NP bacterial cells, which leads to disruption of the cell membrane and thus to increased permeability and cell death (Haghi *et al.*, 2012; Bahjat *et al.*, 2021).

CONCLUSION

The TiO₂ NP was prepared successfully by sol-gel technique at room temperature. Then, the diagnosis and characterization of the TiO₂ NP was carried out. SEM measurement confirmed that the TiO₂ NP is spherical shape, while the wavelength of the TiO₂ NP was 345 nm, which was observed by UV inspection. And through (FTIR) the effective aggregates indicating the presence of NP TiO₂ were known. While the results of the XRD analysis indicate obtaining TiO₂ (NPs) of the rutile type. It was observed in the AFM analysis The TiO₂ NPs are surface rough. The effectiveness of) TiO₂NPs) was tested on types of Gram-positive and negative bacteria, where all types of bacteria used in this research were inhibited with different diameters, and it was noted that the anti-bacterial efficiency increased by increasing the concentration of the (TiO₂NPs) solutions used.

REFERENCES

1. Ahmad, R., Mohsin, M., Ahmad, T., and Sardar, M. (2015). Alpha amylase assisted synthesis of TiO₂ nanoparticles: structural characterization and application as antibacterial agents. *Journal of hazardous materials*, 283, 171-177.
2. Al-Hadedee, L.T. and Awahd, S.A.R.H., (2022). Producing Edible Whey Proteins Films Isolate Incorporated with Silver Nanoparticles and the Mechanical and Antimicrobial Properties. *Indian Journal of Ecology*49 (18), 276-279.
3. Bahjat, H. H., Ismail, R. A., Sulaiman, G. M., and Jabir, M. S. (2021). Magnetic field-assisted laser ablation of titanium dioxide nanoparticles in water for anti-bacterial

- applications. *Journal of Inorganic and Organometallic Polymers and Materials*, 31, 3649-3656.
4. Di Paola, A., Bellardita, M., and Palmisano, L. (2013). Brookite, the least known TiO₂ photocatalyst. *Catalysts*, 3(1), 36-73.
 5. De Oliveira, R. V., van Tilburg, M. F., dos Santos, R. Q., Moreno, F. B., Monteiro-Moreira, A. C. O., and Moura, A. (2014). Effects of cashew nut meal on ram sperm proteins. *Acta Veterinaria Brasilica*, 8, 246-247.
 6. Dai, S., Wu, Y., Sakai, T., Du, Z., Sakai, H., and Abe, M. (2010). Preparation of Highly Crystalline TiO₂ Nanostructures by Acid-assisted Hydrothermal Treatment of Hexagonal-structured Nanocrystalline Titania/Cetyltrimethylammonium Bromide Nanoskeleton. *Nanoscale research letters*, 5, 1829-1835.
 7. Fahem, M. Q., and Hassan, T. A. (2022). Hydrothermal Process to Prepare Novel Phase Titanium Sub-Oxide Ti₆O₁₁ from Nano Rutile Titanium Dioxide Particles with Different Autoclave Reactors. *Iraqi Journal of Science*. 63, 4740-4748
 8. Geethalakshmi, R., and Sarada, D. V. L. (2012). Gold and silver nanoparticles from *Trianthema decandra*: synthesis, characterization, and antimicrobial properties. *International journal of nanomedicine*, 7, 5375-5384.
 9. Ghaly, M. Y., Jamil, T. S., El-Seesy, I. E., Souaya, E. R., and Nasr, R. A. (2011). Treatment of highly polluted paper mill wastewater by solar photocatalytic oxidation with synthesized nano TiO₂. *Chemical Engineering Journal*, 168(1), 446-454.
 10. Hamza, M. A., Khalil, A. S., and Yaseen, H. M. (2013). Synthesis of Yb³⁺ Doped TiO₂ Nano Particles Powder as IR Filter via Sol-Gel. *Advances in Materials Physics and Chemistry*. 3 (4), 214-216
 11. Haggi, M., Hekmatafshar, M., Janipour, M. B., Gholizadeh, S. S., Faraz, M. K., Sayyadifar, F., and Ghaedi, M. (2012). Antibacterial effect of TiO₂ nanoparticles on pathogenic strain of *E. coli*. *International Journal of Advanced Biotechnology and Research*, 3(3), 621-624.
 12. Jaafer, H. I. (2009). Photostability of PMMA-TiO₂ micro composites and PMMA-TiO₂ nano composites. *Iraqi Journal of Physics*, 7(8), 6-10.
 13. Kim, D. H., Hong, H. S., Kim, S. J., Song, J. S., and Lee, K. S. (2004). Photocatalytic behaviors and structural characterization of nanocrystalline Fe-doped TiO₂ synthesized by mechanical alloying. *Journal of Alloys and Compounds*, 375(1-2), 259-264.
 14. Ramalingam, S. (2019). Synthesis of nanosized titanium dioxide (TiO₂) by sol-gel method. *Int. J. Innov. Technol. Explore*. 9, 2278-3075.
 15. Wankhede. S. A. and Barik ,A., (2021). Preparation of Tio₂ Nanoparticles and Its use in Wastewater Treatment, *International Journal of Engineering Research & Technology* 4 (9), 2278-0181
 16. Vijayalakshmi, R., and Rajendran, V. (2012). Synthesis and characterization of nano-TiO₂ via different methods. *Arch. Appl. Sci. Res*, 4(2), 1183-1190.
 17. Yu, J., Su, Y., Cheng, B., and Zhou, M. (2006). Effects of pH on the microstructures and photocatalytic activity of mesoporous nanocrystalline titania powders prepared via hydrothermal method. *Journal of Molecular Catalysis A: Chemical*, 258(1-2), 104-112.